

# 1 **Impact of climate change on European winter and summer flood losses**

2 Maximiliano Sassi<sup>1\*</sup>, Ludovico Nicotina<sup>1</sup>, Pardeep Pall<sup>2</sup>, Dáithí Stone<sup>3,4</sup>, Arno Hilberts<sup>1</sup>, Michael Wehner<sup>3</sup>,  
3 and Stephen Jewson<sup>1</sup>

4 <sup>1</sup>Risk Management Solutions Inc., London, UK

5 <sup>2</sup>University of Oslo, Oslo, Norway

6 <sup>3</sup>Lawrence Berkeley National Laboratory, Berkeley, CA, USA

7 <sup>4</sup>Global Climate Adaptation Partnership, Oxford, UK

8

9 Abstract

10 Climate change is expected to alter European floods and associated economic losses in various ways.  
11 Here we investigate the impact of precipitation change on European average winter and summer financial  
12 losses due to flooding under a 1.5°C warming scenario (reflecting a projected climate in the year 2115  
13 according to RCP2.6) and for a counterfactual current-climate scenario where the climate has evolved  
14 without anthropogenic influence (reflecting a climate corresponding to pre-industrial conditions). Climate  
15 scenarios were generated with the Community Atmospheric Model (CAM) version 5. For each scenario,  
16 we derive a set of weights that when applied to the current climate's precipitation results in a climatology  
17 that approximates that of the scenario. We apply the weights to annual losses from a well-calibrated (to  
18 the current climate) flood loss model that spans 50,000 years and re-compute the average annual loss to  
19 assess the impact of precipitation changes induced by anthropogenic climate change. The method relies  
20 on a large stochastic set of physically based flood model simulations and allows quick assessment of  
21 potential loss changes due to change in precipitation based on two statistics, namely total precipitation,  
22 and total precipitation of very wet days (here defined as the total precipitation of days above the 95<sup>th</sup>  
23 percentile of daily precipitation). We compute the statistics with the raw CAM precipitation and bias-  
24 corrected precipitation. Our results show that for both raw and bias-corrected statistics i) average flood  
25 loss in Europe generally tend to increase in winter and decrease in summer for the future scenario, and  
26 consistent with that change we also show that ii) average flood loss have increased (decreased) for  
27 winter (summer) from pre-industrial conditions to the current day. The magnitude of the change varies  
28 among scenarios and statistics chosen.

29

30 Keywords: climate change, Paris agreement, flood risk, economic loss, anthropogenic climate change,  
31 stochastic precipitation, average flood loss, RCP2.6

32

33 (\*) Risk Management Solutions Ltd, 30 Monument Street, EC3R 8NB, London, United Kingdom,  
34 maximiliano.sassi@rms.com

35

36

37

38 1. Introduction

39 Inland flooding in Europe and worldwide affects the life of millions and causes large economic losses  
40 (Guha-Sapir et al., 2017). The number of severe flood events in Europe has increased over the last 35  
41 years and more than 1500 flood events have been registered in Europe since 1980, half of which  
42 occurred after the year 2000 (EEA, 2017). In the future this trend is expected to continue because of  
43 changes in land use, socio-economic factors and the potential impacts of climatic changes induced by  
44 anthropogenic greenhouse gas emissions (Winsemius et al., 2015). Changes in precipitation patterns and  
45 their extremes under global warming are expected to be one of the major drivers in future flood risk; the  
46 impact of temperature changes on precipitation has been the subject of many scientific contributions over  
47 the last decade leading to a deeper understanding of the mechanisms through which a warmer  
48 atmosphere can lead to changes in the rainfall distribution (Pfahl et al., 2017; O’Gorman and Schneider,  
49 2009; Allan, 2011; Haerter et al., 2010). Specifically, Pfahl et al. (2017) have shown how the response of  
50 extreme rainfall in the presence of temperature changes shows strong spatial variability due to energy  
51 availability in the atmosphere. Although it is widely accepted that precipitation and its extremes are likely  
52 to increase in a warmer world, the same is not true for flood frequency and magnitude. Several studies  
53 have explored long term river flow data sets to identify potential climate change trends showing how the  
54 inhomogeneity of available time series, human influence in shaping the streamflow distributions and  
55 statistical uncertainty do not allow a confident statement on present-day trends in flood peak frequency  
56 and magnitude over time (Mangini et al., 2018; Hodgkins et al., 2017; Bloschl et al., 2017). Therefore,  
57 there is significant uncertainty on the potential impacts of climatic changes on the economic damages  
58 associated with flood risk and there is no consensus yet around the magnitude and spatial distribution of  
59 change of average annual loss (an indicator of flood risk).

60 Projections of future annual precipitation indicate wetting tendencies for Scandinavia and central-eastern  
61 Europe and drying tendencies for the southern parts of Europe (Maraun, 2013). This pattern has been  
62 observed in records of winter extreme precipitation (Donat et al., 2013). A strong increase in winter heavy  
63 precipitation (defined as precipitation above the 99<sup>th</sup> percentile for months December to February) over  
64 Scandinavia and eastern Europe has been reproduced with global climate models (Giorgi et al., 2014)  
65 and regional climate models (Rajczak et al., 2013). In southern parts of Europe, even though mean  
66 precipitation is projected to decrease, heavy precipitation is projected to increase (Sillmann et al., 2013).  
67 These studies generally quantify changes at relatively high levels of global warming (3 °C and more). At  
68 1.5 and 2 °C, King and Karoly (2017) showed increased intensity of extreme wet days (day with highest  
69 one day precipitation total within the season) in both summer and winter, in contrast to a weaker signal for  
70 mean changes over most of the continent. Vautard et al (2014) also found robust increases in mean  
71 winter precipitation in northern Europe, with extreme precipitation increase over eastern Europe and  
72 Scandinavia in summer and over southern Europe in winter. Dosio and Fischer (2018) found that locally  
73 the change in mean precipitation due to further warming is not significant but is accompanied by a robust  
74 change in extreme precipitation.

75 Climate change is expected to alter European flood risk and, specifically, average annual losses in  
76 various ways. Rojas et al. (2013) conducted an ensemble-based pan-European flood hazard assessment  
77 for present and future conditions and found that with no adaptation to climate change the average annual  
78 loss by 2080 with 3 °C global warming (SRES A1B emission scenario) would be about 17 times greater  
79 than in the present; with adaptation the increase would be ten-fold. In earlier studies, Kundzewicz et al.  
80 (2010) showed projected annual losses for the countries in Europe to be between 2 to 10 times greater by  
81 2080 compared to 1970 (again for the SRES A1B scenario), and Ciscar et al. (2011) found the increase in  
82 annual loss from river floods in Europe more than doubles for the same period and employing similar  
83 scenarios. In a recent study which considers natural correlation between events, Jongman et al. (2014)

84 found an almost five-fold increase in annual loss by 2050 for a 3 °C global warming, whereas Alfieri et al.  
85 (2015) found for the same period an increase of 4 to 8 times for a 4 °C global warming scenario. More  
86 recently, Alfieri et al. (2018) reported changes in annual loss for three warming levels (1.5, 2 and 3 °C)  
87 and three independent studies to be roughly in a range between 2 to 4 times of the present. The latter  
88 three studies do not include the effect of future socio-economic changes on population, economy, and  
89 land use, so flood risk was estimated assuming present-day exposure and vulnerability. Because flood  
90 risk is a non-linear function of hazard, exposure, and vulnerability (e.g. de Moel et al., 2015), relative  
91 changes in average annual loss including future adaptation measures and socio-economic impacts due to  
92 climate change can vastly differ. Here we focus on average annual losses that would occur in a world  
93 where only the climatic (i.e. hazard) variables have changed, and particularly the precipitation.

94 Flood risk assessments at pan-European scale under different degrees of warming typically rely on multi-  
95 model ensembles encompassing several climate and hydrological models (e.g. Rojas et al., 2012; Alfieri  
96 et al., 2015; Gosling et al., 2016). Donnelly et al. (2017) compared runoff, discharge, and snowpack in  
97 Europe for climate change at 1.5, 2 and 3 °C global warming above pre-industrial level. They employed  
98 five hydrological models forced with multi-model ensembles of climate projections to calculate changes in  
99 hydrological indicators. They found robust increases in runoff over the Scandinavian mountains and  
100 robust decreases in Portugal at 1.5 °C, with extents further increasing over Norway and Poland and the  
101 Iberian coast, Balkan coast, and parts of the French coast at 3 °C. A robust increase of discharge with  
102 warming level was found only in Scandinavia. Thober et al. (2018) also assessed the impacts of climate  
103 change employing a multi-model ensemble of three hydrological models forced by five Coupled Model  
104 Intercomparison Project Phase 5 (CMIP5) general circulation models (GCMs) under three Representative  
105 Concentration Pathways (RCPs 2.6, 6.0, and 8.5). They found decreases for high flows and annual  
106 maxima in the Mediterranean and Eastern Europe, mostly related to decreases in total annual  
107 precipitation. They also found increases in high flows in Northern regions due to increasing precipitation,  
108 but with annual maxima decreasing due to less snowmelt. Alfieri et al. (2018) compared three studies of  
109 flood hazard and risk projections based on ensemble projections of expected damage and population  
110 affected at country level. They found a substantial increase in flood risk over most of Central and Western  
111 Europe at all warming levels. In this study, we do not attempt to simulate flood risk under climate change  
112 scenarios. Instead, we employ annual losses from a fully calibrated flood model of the current climate and  
113 translate these losses to the future or counterfactual world by reweighting the annual losses. Even though  
114 this approach is simple by design, it relies on a long stochastic set of physically based simulations  
115 produced with a stochastic rainfall generator, which is not the case in the other studies as they normally  
116 use only a hundred years of simulation and extreme value theory for extrapolation to higher return levels.

117 The objective of this study is to present a simple approach to assess potential changes in European flood  
118 risk due to relative changes in precipitation driven by climate change. The proposed approach combines  
119 the potential change in flood risk from river and pluvial flooding due to relative changes in precipitation.  
120 We apply this approach to assess the impact of relative changes in precipitation on European flood  
121 damages for two climate change scenarios produced with the Community Atmospheric Model version 5  
122 (CAM). Precipitation fields are obtained from ensembles generated with CAM for two climate change  
123 scenarios. Scenarios include future global warming at 1.5 °C above pre-industrial conditions, and a  
124 hypothetical present-day counterfactual scenario where the climate has evolved without anthropogenic  
125 influence. The flood risk response to changes in precipitation relies on the RMS European Flood Model: A  
126 Monte Carlo model for the simulation of flood risk in Europe for the insurance market. This model has  
127 been calibrated and validated in its hazard and damage components with the goal to reproduce economic  
128 and insured flood damages and is employed here to evaluate changes in this variable under current  
129 climate. The model uses a probabilistic set of flood events to model flood risk, and the approach adopted  
130 in this study involves the creation of an alternative probabilistic set, by reweighting the stochastic model

131 precipitation to mimic the precipitation statistics of the climate scenarios produced by the GCM. This  
132 paper is organized as follows: Section 2 describes the methods including the model runs, reweighting  
133 method, stochastic precipitation, loss tables and bias-correction methodology; Section 3 describes the  
134 relative changes in two precipitation statistics for the scenarios using raw input and bias-corrected input,  
135 along with the loss changes; Section 4 discusses the results; Section 5 concludes this paper.

## 136 2. Methods

137 In the present work we assess the impact of climate change on flood risk by incorporating a climate  
138 change signal, derived from state-of-the-art climate model simulations (Section 2.1) into a European  
139 probabilistic flood loss model (Section 2.2). The coupling of the models is done by means of a  
140 methodology devised to apply the spatially variable climate change signal to the stochastic flood losses  
141 produced by the RMS European Flood Model for the present climate (Section 2.3). Given the large  
142 uncertainties involved in climate model outputs and in modelling the hydrologic response in a changing  
143 climate (highlighted in the wide literature review discussed above) this paper focuses on the impact of  
144 precipitation changes and applies these to a time series of modelled European flood losses. This  
145 simplified approach, whilst not targeting changes in the frequency and magnitude of extreme events and  
146 their effect on the tail of the economic loss distribution, allows to represent the potential effect of changes  
147 in wetness condition over the continent which are reflected on the average annual loss (ie. the mean of  
148 the flood loss distribution).

### 149 2.1. Climate model runs

150 Simulations were carried out with CAM version 5.3 (Neale et al. 2010), a dynamical model of the  
151 atmosphere run at approximately quarter degree spatial resolution (Wehner et al. 2018) under the  
152 protocols of the Half a Degree Additional warming, Prognosis, and Projected Impacts (HAPPI) experiment  
153 (Mitchell et al. 2017) and of the C20C+Detection and Attribution Project (Stone et al. in preparation).  
154 (Note the model is listed as “CAM5.1.2-0.25degree” under the archive portal for both projects. See  
155 <http://portal.nersc.gov/c20c/>). The HAPPI project was designed to provide model output data describing  
156 climate and weather changes under stabilized 1.5 and 2.0°C levels of global warming, as compared to  
157 preindustrial conditions (1861-1880). CAM was run under three time-slice experiments to generate five  
158 10-year simulations for the present climate (2006-2015) and six simulations each for potential future  
159 climate under stabilized 1.5°C and 2°C levels of global warming (nominally 2106-2115). We use daily  
160 resolution output in this paper.

161 Present climate simulations include observed forcing conditions for sea surface temperatures (SSTs) and  
162 sea-ice cover. Each simulation differs from the others in the initial weather state, and they are limited to  
163 10 years in length to avoid long-term trends dominating the variability. The 2006-2015 runs use realistic  
164 observation-based time-varying conditions for all climate drivers during that time. These drivers are  
165 atmospheric greenhouse gas concentrations, tropospheric aerosol concentrations, atmospheric ozone  
166 concentrations, solar luminosity, SSTs, and sea-ice cover. SSTs in scenarios of the future are prescribed  
167 by summation of the observed 2006-2015 SSTs and an offset, estimated between decadal-averages of  
168 the 2006-2015 period and the projected warmer global conditions for the 2091-2100 period (Mitchell et al.  
169 2017). The 1.5°C scenario was constructed following SST warming according to the response to the  
170 RCP2.6 in CMIP5 model simulations (which results in a global warming of approximately 1.5°C), with sea  
171 ice concentration modified accordingly. Greenhouse gas, aerosol, and ozone concentrations are set  
172 according to RCP2.6. More implementation details can be found in Mitchell et al. (2017) and Wehner et  
173 al. (2018).

174 An additional set of four 10-year simulations corresponds to the counterfactual historical scenario of the  
175 C20C+ Detection and Attribution project (Stone et al. in preparation). This 'naturalised' climate scenario  
176 represents hypothetical counterfactual time-varying conditions for climate drivers during the 2006-2015  
177 period whereby industrial anthropogenic emissions had not occurred over the course of history. It is  
178 constructed by setting the Present-scenario greenhouses gases, aerosols, and ozone to pre-industrial  
179 (year 1855) values and adjusting SSTs and sea ice accordingly. The SST adjustment is based on the  
180 difference of temperatures from CMIP5 climate models run with and without anthropogenic influence  
181 (Stone and Pall in preparation). Here we will make use of the natural scenario simulations as well as  
182 those for present climate and future climate at 1.5°C global warming, we will refer to these simulations as  
183 NAT, Present and Plus15, respectively.

184 Modelled precipitation is bias-corrected with respect to observations (E-OBS, Haylock et al, 2008) for the  
185 period 1961-2011, using quantile mapping. Specifically, we adopt a non-parametric approach, termed  
186 quantile delta mapping (Cannon et al., 2015). First, future (or natural) climate model outputs are bias  
187 corrected to observations by quantile mapping. Second, model-projected relative changes in quantiles are  
188 superimposed on the bias-corrected model outputs. The method preserves model-projected relative  
189 changes in quantiles, while at the same time correcting systematic biases in quantiles of a modeled  
190 series with respect to observed values – one of the reasons for discrepancy in flood risk assessments, as  
191 pointed out by Thober et al. (2018).

## 192 2.2. The RMS European Flood Model

193 The RMS European Inland Flood Model is a probabilistic, high resolution, flood catastrophe model that is  
194 widely used in the insurance industry to estimate flood risk for a given portfolio of insured exposures. The  
195 model currently covers 15 countries: Austria, Belgium, Czech Republic, France, Germany, Hungary,  
196 Ireland, Italy, Liechtenstein, Luxembourg, Monaco, Poland, Slovakia, Switzerland, and the United  
197 Kingdom. In this study we exclude the Republic of Ireland, Italy, and Northern Ireland, which were under  
198 development while doing this analysis, and we also exclude Liechtenstein, Luxemburg, and Monaco  
199 because of their small size relative to the model domain. The model includes three main components: a  
200 hazard module, a damage module, and a financial module. The hazard module simulates precipitation-  
201 driven flood risk and risk from major river flooding with a physically based approach. The damage module  
202 relies on detailed building inventories and a comprehensive catalogue of damage functions to describe  
203 the vulnerability of buildings to flood risk. The financial model quantifies the economic loss of exposure to  
204 flooding.

205 Here we focus on the hazard module and the methodology used to simulate probabilistic flood risk maps  
206 from a stochastic rainfall simulation. The flood hazard model relies on a continuous 50,000-year Europe-  
207 wide stochastic precipitation dataset which has been generated with a stochastic rainfall generator based  
208 on the main modes of variability of gridded precipitation data through Principal Component Analysis  
209 (Bouvier et al., 2003; Westra et al., 2007). Observed gridded precipitation (E-OBS, Haylock et al., 2008)  
210 was available for the period 1961-2011 (daily resolution at quarter-degree spatial resolution) while the  
211 other atmospheric variables relevant for runoff generation were obtained from the GLDAS dataset  
212 (<https://ldas.gsfc.nasa.gov/gldas/>) for the same period (3 hourly resolution at one-degree spatial  
213 resolution).

214 Stochastic monthly rainfall fields, obtained as a linear combination of stochastic Principal Components  
215 (PCs) and main modes of variability of the monthly rainfall anomalies (EOFs), were subsequently  
216 disaggregated in space and time to 3-hourly, 6km resolution grids. Spatial disaggregation was performed  
217 through the scaling properties of standardized rainfall fluctuations with statistical scaling parameters  
218 related to elevation and convective available potential energy (CAPE) (Perica and Foufoula-Georgiou,

219 1996). Temporal disaggregation is performed through a bootstrapping methodology. The stochastic  
220 rainfall generator considers the relationship between rainfall and the state of the atmosphere by  
221 incorporating the correlation between the rainfall principal components and the North Atlantic Oscillation  
222 (NAO), which is simulated in the stochastic model as an AR (1) process calibrated on monthly NAO data  
223 in the available observation period (data from National Weather Service <http://www.cpc.ncep.noaa.gov/>).

224 The modelling domain is subdivided into 8546 catchments, based on standard catchment delineation  
225 routines (Metz et al., 2011); catchment size varies between 50 and 500 km<sup>2</sup>. Rainfall-runoff processes are  
226 modelled with a semi-distributed rainfall-runoff approach based on TOPMODEL (Beven and Freer, 2001),  
227 with a runoff generation module that accounts for evapotranspiration, canopy interception, snow  
228 accumulation and melting, formulated by 15 parameters. The hydrological model is calibrated to  
229 observations for approximately 2000 gauges employing time series of up to 30 years in length (minimum  
230 10 years) using a genetic algorithm to appropriately cover the parameter space (Deb et al., 2002). We  
231 employ two cost functions in the optimization, one for the overall bias and another for the discharge  
232 peaks. After performance assessment we retain about 1400 gauges. Parameters are redistributed to  
233 upstream catchments when gauges are not available. Discharge at the outlet of the catchments is  
234 obtained through the Muskingum-Cunge routing technique. Again, we perform calibration of the routing  
235 model for the same gauges. The model is therefore designed to capture the temporal evolution (e.g.  
236 antecedent conditions and clustering of events) and the spatial correlation of inland flood risk within and  
237 between countries.

238 We employ a 50 m resolution digital terrain model (DTM) for computing flood depths on major rivers as  
239 well as surface flooding induced by precipitation. Manning coefficients are obtained from land use land  
240 cover data (<https://land.copernicus.eu/pan-european/corine-land-cover>). We compute fluvial and pluvial  
241 inundation maps for several return periods using the river discharge and surface runoff, respectively.  
242 Inundation maps are obtained by solving the shallow water equations. More details about model  
243 implementation and validation can be found in Zanardo et al. (2019).

244 The time sequence of flood damages is obtained in the form of a Monte Carlo set of stochastic flood  
245 events resulting from the estimation of economic damages to buildings, for a given portfolio of exposed  
246 assets. The damage simulation is performed at the building level by leveraging the high-resolution flood  
247 maps and a detailed model of the building stock and their vulnerabilities to a given level of flood depth.  
248 The results of the Monte Carlo simulation are outputted to a year-loss table (YLT), where each simulated  
249 year has a uniform probability of occurrence equal to the inverse of the length of the simulation. The  
250 model contains an average of about 30 damage producing flood events per year over the 50,000 years of  
251 simulation. The 30 events are domain wide and a single event can affect multiple countries. For example,  
252 the UK has 4.2 events per year. Each event is identified with time and date, duration, and location. We  
253 compute the annual loss by aggregating the loss of events occurring in each year. The average annual  
254 loss (normally referred as AAL) is obtained by computing the mean of the annual losses over the length of  
255 the simulation. Note that in this paper we make the distinction of winter and summer losses, in which case  
256 the annual loss is based on winter and summer events separately.

257

### 258 2.3. Reweighting method

259

260 We present a method to derive a set of weights that, when applied to a given statistic of the stochastic  
261 precipitation dataset, produces a climatology that approximates the statistic of an imposed climate  
262 change scenario. We then apply the weights to the YLT and re-compute the AAL to assess the loss  
263 change due to precipitation under climate change. Here we introduce the method in terms of yearly  
264 calculations whereas in the results section we will adopt a seasonal approach, in which case, the

265 statistics are computed separately for each season of each year and similarly, for the losses. We compute  
266 two statistics: total precipitation (SUM) is the sum of all days that belong to the year; and the contribution  
267 of very wet days to the total precipitation (R95pTOT), here defined as the sum of all days with  
268 precipitation greater than the 95<sup>th</sup> percentile of the daily precipitation.

269  
270 In the following,  $p_{cy}$  is the stochastic precipitation statistic for catchment  $c$  and year  $y$  and  $p_c$  is the  
271 reference climatological mean of the statistic for catchment  $c$ . If the mean precipitation statistic varies  
272 linearly with time, the expected value  $N$  years from the reference period is given by

273 (Equation 1)

274 with  $k_c$  the annual rate of change in the statistic for catchment  $c$ . We derive a set of annual weights  $\omega_y$ ,  
275 such that when the mean precipitation statistic is calculated using the weighted  $\omega_y p_{cy}$ , the latter  
276 approximates the expected value given by the above equation. The  $p_c$  quantities are computed for each  
277 year in the stochastic precipitation dataset whereas the rate of change  $k_c$  is computed as the long-term of  
278 lumped climate model simulations.

279 The approach to obtain the weights involves two steps: first, for each year in the stochastic precipitation  
280 we calculate a climate change index  $\lambda_y$ . This index gives the year relative to the reference period for  
281 which the chosen climate change scenario most closely resembles a given year in the stochastic  
282 precipitation. The reference period here is 1961-2011 and corresponds to the observation period over  
283 which measured rainfall data were available for the creation of the European Flood HD model's stochastic  
284 precipitation set. The minimization is performed across all catchments:

285 (Equation 2)

286 where  $A_c$  is the catchment area and  $\sigma_c$  is the standard deviation of the precipitation statistic of catchment  
287  $c$ . We normalize with the standard deviation to avoid high-precipitation catchments dominating the terms  
288 in the summation. Because  $\lambda_y$  does not depend on  $c$ , the value that minimizes the expression can be  
289 found analytically and is given by:

290 (Equation 3)

291 Second, we find the weights  $\omega_y$  that minimize the following expression:

292 (Equation 4)

293 where  $N_Y$  is the number of years (or individual seasons) in the stochastic precipitation. We use the  
294 climate change index  $\lambda_y$  to inform the weight function  $\omega_y$ . The expression above is optimized numerically  
295 to allow for weight functions of different types.

296 Here, we employ a two-parameter function such that  $f(\lambda_y)$  for positive  $\lambda_y$  and  
297 for negative  $\lambda_y$ , with  $\alpha_1$  and  $\alpha_2$  two positive scalars. The two-parameter function allows for different  
298 weights in the two regions of the frequency domain above and below unity; this means that weighting  
299 towards drier years can have a different scale coefficient than weighting towards wetter years.

300

### 301 3. Results

302 To compare results between the different climate scenarios, simulations within the respective ensembles  
303 are first concatenated. This results in 50-year time series in the case of the future to present comparison  
304 (5 simulations of 10 years each for Plus15 and Present), and 40-year time series in the case of the  
305 natural to present comparison (4 simulations of 10 years each for NAT and Present). We compute all  
306 quantities for winter (DJF) and summer (JJA) seasons.

#### 307 3.1.1. Mean seasonal precipitation

308

309 When compared with E-OBS precipitation, the CAM generally tends to overestimate precipitation in winter  
310 months and underestimate precipitation in summer months (Figure 1). The winter bias can be seen  
311 mainly in mountainous areas; Barcikowska et al. (2018) argues that these differences can be due to both  
312 model and observational biases because observations are less representative in orographic conditions  
313 and because topography is too smooth in the comparatively lower resolution model. However, the  
314 general large-scale wet bias particularly over western Europe could also be indicative of stronger zonal  
315 winds in the model, suggesting more storminess and moisture brought particularly into the UK, Benelux,  
316 and Germany. The summer bias may be explained by insufficient resolution in the model to capture heavy  
317 convective storms, particularly in inland and mountainous regions.

318

319 At 1.5 °C global warming winter precipitation is generally greater throughout Europe compared to the  
320 present; summer precipitation shows slightly wetter conditions in Eastern Europe and drier in Northern  
321 Europe. These results agree with a consensus towards wetter winters in most parts of Europe. The  
322 present to natural comparison mostly shows wetter conditions in winter and drier in summer, which is akin  
323 to the future to present comparison since in the present the climate is generally warmer than in the  
324 naturalised scenario.

325

#### 326 3.2. Relative changes in precipitation statistics

327 Relative changes are computed with respect to present climate simulations. Figure 2 shows the spatial  
328 distribution of the relative changes of the two winter statistics for the two climate change scenarios. The  
329 Plus15 scenario generally shows positive changes throughout Europe and with the largest magnitudes of  
330 the two scenarios. The NAT scenario shows mostly negative changes for eastern Europe and some small  
331 areas with positive changes in western Europe, particularly for R95pTOT. Each scenario shows a smooth  
332 spatial pattern for the total precipitation and a slight increase in patchiness and spikiness for the total  
333 precipitation from very wet days. This could be attributed to sampling uncertainty because given the same  
334 amount of underlying data, extreme metrics are less well sampled than the total. Additionally, since  
335 patchiness is concentrated toward southern Europe, we hypothesize that there may be an increased  
336 influence of convective cells producing patchy extreme precipitation embedded within large-scale  
337 southerly flow due to a warmer Mediterranean under climate warming. In general, patterns are spatially  
338 coherent for the different statistics and do not change sign, however, magnitudes generally tend to  
339 decrease when looking at the more extreme statistics.



340 Figure 3 shows the spatial distribution of the relative changes of the two summer statistics for the two  
341 climate change scenarios. Gray areas indicate areas with too few rainy days to compute a meaningful  
342 change. Relative changes can easily be greater than 100% because summer precipitation is generally  
343 noisier than winter precipitation (we have capped these to avoid extending the limits in the color bar  
344 plots). Patchiness is much more characteristic in the summer spatial patterns too. Like winter, spatial  
345 patterns are generally coherent when looking at the different statistics. The 1.5°C scenario generally  
346 shows a tendency for drier conditions in northern Europe and parts of Italy, whereas both statistics seem  
347 to agree on wetter conditions over southern and Eastern Europe. These results are not in full agreement  
348 with previously published results. Reasons for discrepancy could have to do with scenario design and  
349 model resolution. In terms of scenario design, most of the studies mentioned in the introduction concern  
350 about +1% CO<sub>2</sub> per year emissions scenarios, where CO<sub>2</sub> increases dominate any aerosol changes. The  
351 Plus15 scenario exhibits an aggressive CO<sub>2</sub> ramp-down and aerosol ramp-down, where the effects of  
352 any aerosol ramp-down rival that of any further CO<sub>2</sub> increase. The NAT scenario also shows drier  
353 conditions over northern Europe, and wetter conditions over eastern Europe, France, and parts of the UK.

354 We bias-correct the CAM simulations by preserving the relative change in precipitation quantiles of  
355 modelled precipitation (i.e. trend in modelled projections, see Figure 4). The bias correction is performed  
356 for winter and for summer separately, and for days with precipitation greater than 1 mm/day only to avoid  
357 changing the wet/dry sequence of the underlying precipitation. Figure 5 shows spatial plots of the mean  
358 seasonal precipitation difference between scenarios, after bias-correction. Spatial patterns are  
359 comparable to those before bias-correction and differences between scenarios tend to be smaller. Some  
360 areas of high precipitation in Plus15 (e.g. France), particularly for winter, are missing after bias-correction.  
361 Summer changes for Plus15 indicate drier conditions in GB and Benelux. Winter spatial patterns in the  
362 relative change of both statistics after bias-correction (Figure 6) are very similar to the ones computed  
363 with the raw precipitation. In the summer (Figure 10), spatial patterns before and after bias correction also  
364 compare well.

### 365 3.3. Relative changes in average annual loss

366 In what follows we present the negated results for the NAT scenario so that both Plus15 and NAT  
367 scenarios appear with the same sign in the plot. Figure 8 shows the relative change in winter AAL  
368 obtained with the raw and bias-corrected (BC) winter precipitation statistics and both climate change  
369 scenarios, for the EUFL domain and split by country. The Plus15 scenario results in a positive loss  
370 change with both statistics; R95pTOT generally yields a lower magnitude, which is a direct consequence  
371 of the smaller relative change of R95pTOT compared to the total precipitation (Figure 6). The NAT  
372 scenario shows reduced magnitudes in the relative change of the AAL by country and for the entire  
373 domain when compared to the Plus15 scenario. This is because the relative changes of both statistics in  
374 the NAT scenario are milder than in the Plus15 scenario. Discrepancies in AAL change arising from both  
375 statistics are minor in the NAT scenario, generally showing a slightly higher magnitude with R95pTOT.

376 Summer changes in AAL (Figure 7) generally show an opposing trend for the two climate change  
377 scenarios, except for France in the Plus15 scenario that shows a positive trend with the bias-corrected  
378 total precipitation. Magnitudes of the summer AAL change in the Plus15 scenario can be compared with  
379 winter; however, summer AAL changes are generally more sensitive to R95pTOT than in winter, showing  
380 greater changes in AAL. The NAT scenario shows greater magnitudes of loss change when compared to  
381 winter. These observations stem from the fact that in general winter changes are spatially smooth  
382 compared to summer changes (Figures 6 and 7); for summer we observe positive and negative changes  
383 within the domain, and even within countries. Furthermore, summer changes in statistics show greater  
384 magnitudes and more patchy features. It is important to note that for winter differences between SUM and  
385 R95pTOT are less prominent than for summer.

386 4. Discussion

387 The method we presented assumes that the precipitation statistic varies linearly with time from the  
388 present to the time where the climate change scenario applies (either future or pre-industrial). This may  
389 limit the application of the method if we consider a hypothetical timeline where global warming, and the  
390 precipitation response to that warming, displays a non-linear trajectory. For instance, this is the case of  
391 the 2°C global warming (Plus20) simulations of the HAPPI project (Barcikowska et al., 2018; Li et al.,  
392 2018). One way of circumventing this limitation would be to compute the changes in AAL by splitting the  
393 timeline into two (or more) parts: first compute the changes from Present to Plus15, then apply the  
394 weights to Present conditions to obtain a stochastic precipitation for Plus15 climate, and finally compute  
395 the changes from Plus15 to Plus20. This results in double-weighting the reference loss estimate. The  
396 limitation of this method is that the intermediate stochastic precipitation results from an approximation of  
397 the projected climate and further iterations would necessarily imply an accumulation of errors that may  
398 render subsequent loss estimates less accurate.

399 Our methodology relies on the assumption that precipitation alone is a good indicator of changes in the  
400 flood loss distribution. This is certainly a simplifying assumption considering that other climatological  
401 drivers are likely to have an impact as well (Kay et al. 2011; Schaller et al. 2016), and that feedback  
402 mechanisms may exist that are unaccounted for (e.g., increasing mean temperatures leading to  
403 increasing evapotranspiration). However, because precipitation acts as a first-order control on flood  
404 losses, we believe the approximations made in this paper still provide useful insights. Although at event  
405 level, changes in precipitation cannot directly be translated to changes in inundation patterns and flood  
406 losses, we believe that the methodology proposed is suitable to capture changes in wetness conditions  
407 that translate into an increased/decreased propensity to flooding. Given the non-linearities involved we  
408 suggest that these insights should be translated into an average annual loss change rather than impacts  
409 on the full probability distribution of flood losses.

410 Furthermore, the assumptions made need to be evaluated in the context of other approximations in  
411 similar research. The observation that a full-fledged impact assessment of climate change on flood risk  
412 can carry significant uncertainty due to factors such as climate model choice (Deser et al., 2012),  
413 downscaling and bias-correction procedures, hydrological model choice and parameter estimation  
414 (Donnely et al., 2017) are examples of such approximations. Moreover, Alfieri et al. (2018) concluded that  
415 climate projections are the main driver influencing future trends of flood risk under global warming  
416 because model error is small than the difference between different scenarios of future climate change.  
417 These factors are further complicated by a small number of flood events, as they correspond to climate  
418 simulations that typically span no more than 100 years, similarly to the observed record. Because flood  
419 loss time series have a large natural variability, the estimation of an AAL based on a relatively short  
420 record (e.g., less than 100 samples) of annualised losses also introduces considerable sampling error. In  
421 our case, a fully-fledged approach would require bias-correcting the precipitation and the other  
422 atmospheric variables to generate a stochastic dataset that is consistent with the one employed in the  
423 RMS European Flood HD Model.

424 In addition to the already mentioned unmodelled feedbacks, the AAL estimates presented here do not  
425 consider the effects of adaptation and other indirect socio-economic impacts and are based on the  
426 potential change in the flood hazard only. Population projections suggest that EU population has a mild  
427 decreasing trend (UN report, 2017). Jongman et al. (2012) suggest a constant or decreasing exposed  
428 population but an increase in exposed assets. The assumptions in this study allow for a reduction of the  
429 uncertainty involved in the modelling exercise (eg. bias correction of multiple meteorological variables  
430 from the climate model output, uncertainties in simulating the hydrologic response under varying climate,

431 uncertainties in the estimate of socio-economic changes) and therefore to investigate the connection  
432 between projected changes in precipitation and projected changes in loss. On the other hand they do not  
433 allow us to investigate the full probability distribution of financial losses and the effect of potential changes  
434 in the frequency of extremes and the effect of future changes of population and/or economic assets which  
435 would likely have a positive effect on AAL. In a recent study on paired flood events, Kreibich et al. (2017)  
436 showed that the lower damage caused by a second event was mainly due to significant reductions in  
437 vulnerability via raised risk awareness, preparedness, and improvements of organizational emergency  
438 management. Furthermore, the observed increase in flood damage in many regions of the world is  
439 generally dominated by exposure increase (e.g. Bouwer, 2011), so it is possible a balance between the  
440 effects of exposure and vulnerability that could eventually cancel each other out in the future.

441 We conducted a sensitivity analysis into the effect of raising defences, based on current adaptation  
442 literature (Alfieri et al., 2016). The AAL for winter and summer together is reduced by about 2, 12 and  
443 20% for an increase in the defence return period standard of protection of 5, 25 and 50% respectively. If  
444 we assume these adaptation measures occur within the coming 50-100 years, the values obtained here  
445 are comparable to the changes in AAL that we estimate are due to climate change only. Although it is  
446 unlikely all countries in Europe would have raised their standard of protection at the same rate, more  
447 complicated adaptation scenarios could be easily assessed under the proposed evaluation setup.

## 448 5. Conclusions

449 Climate change threatens to increase the frequency and magnitude of high precipitation events with an  
450 associated risk for flood insurance. This has the potential to lead to year-on-year increase in the cost of  
451 flood insurance. In this contribution we assess the potential impact of climate change on Average Annual  
452 Loss (AAL) due to floods. We consider two climate change scenarios: one corresponding to a 1.5 °C  
453 global warming above pre-industrial level, and one corresponding to a naturalised world where climate  
454 has evolved without anthropogenic effects. We introduce a framework to reweight the current precipitation  
455 patterns such that the resulting climatology matches with the future or naturalised precipitation  
456 climatology. Climatology is understood here as the long-term mean of any precipitation statistic (here the  
457 total precipitation and the total precipitation of wet days, for raw and bias-corrected climate model  
458 simulations). The weights were determined by minimization of the squared root differences at catchment  
459 level and apply to the entire model domain and for each simulated year. We employed the weights to  
460 scale the annual loss of events simulated with an in-house European Flood HD model, which is a fully  
461 calibrated (to current climate) flood loss model which consists of a 50,000 year-long stochastic simulation.  
462 Based on derived weights, the annualized losses were weighted and a corresponding AAL was  
463 calculated, to assess the impacts of climate change on flood losses. AAL estimates vary with scenario  
464 and precipitation statistic used, with magnitudes typically within 5% per decade for winter and 10% for  
465 summer. AAL for the future scenario generally tends to increase in winter and decrease in summer,  
466 although the latter shows a magnitude differences when considering the different precipitation statistics.  
467 For the naturalised scenario, flood losses in winter are lower than for current-day conditions, and for  
468 summer they are larger; magnitudes of change are comparable to the magnitude of change between  
469 current-day losses and those for the future scenario. These results are consistent for both raw and bias-  
470 corrected precipitation statistics. Moreover, our results show that adaptation measures (included here as  
471 updates to the current standard of protection of the flood defences) in an idealised scenario that does not  
472 require a cost benefit analysis, could potentially play a role in reducing climate change impacts on  
473 European flood risk.

474

475 Acknowledgements

476 This material is based upon work supported by the U.S. Department of Energy, Office of Science, Office  
477 of Biological and Environmental Research, under contract number DE-AC02-05CH11231. We  
478 acknowledge the E-OBS data set from the EU-FP6 project ENSEMBLES ([http://ensembles-  
eu.metoffice.com](http://ensembles-<br/>479 eu.metoffice.com)) and the data providers in the ECA&D project (<http://www.ecad.eu>).

480  
481  
482  
483  
484  
485  
486  
487  
488  
489  
490  
491  
492  
493  
494  
495  
496  
497  
498  
499  
500  
501  
502  
503  
504  
505  
506  
507  
508  
509  
510  
511  
512  
513  
514  
515  
516  
517  
518  
519  
520  
521  
522  
523

524 References

- 525 Alfieri L, Burek P, Feyen L, and Forzieri G, 2015. Global warming increases the frequency of river floods  
526 in Europe, *Hydrol. Earth Syst. Sci.*, 19:2247–60, 10.5194/hess-19-2247-2015
- 527 Alfieri L, Feyen L, and Di Baldassarre G, 2016. Increasing flood risk under climate change: a pan-  
528 European assessment of the benefits of four adaptation strategies, *Climatic Change*, 136:507–521,  
529 10.1007/s10584-016-1641-1
- 530 Alfieri L, Dottori F, Betts R, Salamon P, and Feyen L, 2018. Multi-Model Projections of River Flood Risk in  
531 Europe under Global Warming, *Climate*, 6, 16, 10.3390/cli6010016
- 532 Allan R, 2011. Climate change: Human influence on rainfall, *Nature*, 470:344–345, 10.1038/470344a
- 533 Barcikowska M, Weaver S, Feser F, Russo S, Schenk F, Stone D, Wehner M, and Zahn M, 2018. Euro-  
534 Atlantic winter storminess and precipitation extremes under 1.5°C versus 2°C warming scenarios, *Earth*  
535 *Syst. Dynam.*, 9:679-699, 10.5194/esd-9-679-2018
- 536 Beven K, and Freer J, 2001. A dynamic TOPMODEL, *Hydrological Processes*, 10.1002/hyp.252
- 537 Blöschl G, Hall J et al., 2017. Changing climate shifts timing of European floods, *Science*, 357:588-590,  
538 10.1126/science.aan2506
- 539 Bouvier C., Cisneros L., Dominguez R., Laborde J-P., Lebel T, 2003. Generating rainfall fields using  
540 principal components (PC) decomposition of the covariance matrix: a case study in Mexico City, *Journal*  
541 *of Hydrology*, 278(1-4): 107-120, 10.1016/S0022-1694(03)00122-7
- 542 Bouwer L, 2011. Have disaster losses increased due to anthropogenic climate change? *Bull. Am. Meteorol.*  
543 *Soc.*, 92(1), 39–46, 10.1175/2010BAMS3092.1
- 544 Cannon A, Sobie S, and Murdock T, 2015. Bias correction of GCM precipitation by quantile mapping: how  
545 well do methods preserve changes in quantiles and extremes? *Journal of Climate*, 28(17), 10.1175/JCLI-  
546 D-14-00754.1
- 547 Ciscar J, Iglesias A, Feyen L, Szabó L, van Regemorter D, Amelung B, Nicholls R, Watkiss P, Christensen  
548 O, Dankers O, Garrote L, Goodess C, Hunt A, Moreno A, Richards J, and Soria A, 2011. Physical and  
549 economic consequences of climate change in Europe, *Proceedings of the National Academy of Sciences*,  
550 108(7):2678-2683; 10.1073/pnas.1011612108
- 551 Deb K, Pratap A, Agarwal S, and Meyarivan T, 2002. A fast and elitist multiobjective genetic algorithm:  
552 NSGA-II, *IEEE Transactions on Evolutionary Computation*, 6(2):182-197; 10.1109/4235.996017
- 553 Deser C, Phillips A, Bourdette V, and Teng H, 2012. Uncertainty in climate change projections: the role of  
554 internal variability, *Clim. Dynam.*, 38:527–546, 10.1007/s00382-010-0977-x
- 555 de Moel H, Jongman B, Kreibich H, Merz B, Penning-Rowsell E, and Ward P, 2015. Flood risk  
556 assessments at different spatial scales, *Mitig Adapt Strateg Glob Change*, 20(865), 10.1007/s11027-015-  
557 9654-z
- 558 Donat M, and Coauthors, 2013. Updated analyses of temperature and precipitation extreme indices since  
559 the beginning of the twentieth century: The HadEX2 dataset, *J. Geophys. Res. Atmos.*, 118:2098–2118,  
560 10.1002/jgrd.50150

561 Donnelly C, Greuell W, Andersson J, Gerten D, Pisacane G, Roudier P, and Ludwig F, 2017. Impacts of  
562 climate change on European hydrology at 1.5, 2 and 3 degrees mean global warming above preindustrial  
563 level, *Climatic Change*, 143:13–26, 10.1007/s10584-017-1971-7

564 Dosio A, and Fischer E, 2018. Will Half a Degree Make a Difference? Robust Projections of Indices of  
565 Mean and Extreme Climate in Europe Under 1.5°C, 2°C, and 3°C Global Warming, *Geophysical*  
566 *Research Letters*, 45, 10.1002/2017GL076222

567 European Environment Agency, 2017. Climate change, impacts and vulnerability in Europe 2016 – An  
568 indicator-based report, EEA Report N.1/2017, ISSN: 1977-8449

569 Giorgi F, Coppola E, and Raffaele F, 2014. A consistent picture of the hydroclimatic response to global  
570 warming from multiple indices: Models and observations, *Journal of Geophysical Research: Atmospheres*,  
571 119(20), 11:695–708, 10.1002/2014JD022238

572 Gosling S, and coauthors, 2016. A comparison of changes in river runoff from multiple global and  
573 catchment-scale hydrological models under global warming scenarios of 1 °C, 2 °C and 3 °C, *Clim.*  
574 *Change*, 141:577–95, 10.1007/s10584-016-1773-3

575 Guha-Sapir D, Below R, and Hoyois P, 2017. EM-DAT: The Emergency Events Database ([www.emdat.be](http://www.emdat.be))

576 Haerter J, Berg P, and Hagemann S, 2010. Heavy rain intensity distributions on varying time scales and  
577 at different temperatures, *Journal of Geophysical Research*, 115, D17102, 10.1029/2009JD013384

578 Haylock M, Hofstra N, Klein Tank A, Klok A, Jones P, and New M, 2008. A European daily high- resolution  
579 gridded data set of surface temperature and precipitation for 1950–2006, *J. Geophys. Res.*, 113, D20119,  
580 10.1029/2008JD010201

581 Hodgkins G, and coauthors, 2017. Climate-driven variability in the occurrence of major floods across  
582 North America and Europe, *Journal of Hydrology*, 552, 10.1016/j.jhydrol.2017.07.027

583 Jongman B., Ward P.J. and Aerts J, 2012. Global exposure to river and coastal flooding: Long term trends  
584 and changes, *Global Environmental Change*, Volume 22, Issue 4

585 Jongman B, Hochrainer-Stigler S, Feyen L, Aerts J, Mechler R, Wouter Botzen W, Bouwer L, Pflug G,  
586 Rojas R, Ward P, 2014. Increasing stress on disaster-risk finance due to large floods, *Nature Climate*  
587 *Change*, 4:264–268, 10.1038/nclimate2124

588 Kay, A. L., S. M. Crooks, P. Pall, and D. A. Stone. 2011. Attribution of Autumn/Winter 2000 flood risk in  
589 England to anthropogenic climate change: a catchment-based study. *Journal of Hydrology*, 406, 97-112,  
590 10.1016/j.jhydrol.2011.06.006

591 King A, and Karoly D, 2017. Climate extremes in Europe at 1.5 and 2 degrees of global warming, *Environ.*  
592 *Res. Lett.*, 12, 114031, 10.1088/1748-9326

593 Kreibich H, and coauthors, 2017. Adaptation to flood risk: Results of international paired flood event  
594 studies, *Earth's Future*, 5:953–965, 10.1002/2017EF000606

595 Kundzewicz Z, Luger N, Dankers R, Hirabayashi Y, Döll P, Pińskwar I, Dysarz T, Hochrainer S, and  
596 Matczak P, 2010. Assessing river flood risk and adaptation in Europe — review of projections for the  
597 future, *Mitig Adapt Strateg Glob Change*, 15: 641, 10.1007/s11027-010-9213-6

598 Li C, Michel C, Seland Graff L, Bethke I, Zappa G, Bracegirdle T, Fischer E, Harvey B, Iversen T, King M,  
599 Krishnan H, Lierhammer L, Mitchell D, Scinocca J, Shiogama H, Stone D, and Wettstein J, 2018.  
600 Midlatitude atmospheric circulation responses under 1.5 and 2.0 °C warming and implications for regional  
601 impacts, *Earth Syst. Dynam.*, 9:359-382, 10.5194/esd-9-359-2018

602 Mangini W, Viglione A, Hall J, Hundecha Y, Ceola S, Montanari A, Rogger M, Salinas J, Borzì I, and  
603 Parajka J, 2018. Detection of trends in magnitude and frequency of flood peaks across Europe,  
604 *Hydrological Sciences Journal*, 63:4, 493-512, 10.1080/02626667.2018.1444766

605 Maraun D, 2013. When will trends in European mean and heavy daily precipitation emerge?  
606 *Environmental Research Letters*, 8(1), 14004, 10.1088/1748-9326/8/1/014004

607 Metz M, Mitasova H, and Harmon R, 2011. Efficient extraction of drainage networks from massive, radar-  
608 based elevation models with least cost path search, *Hydrol. Earth Syst. Sci.*, 15:667-678, 10.5194/hess-  
609 15-667-2011

610 Mitchell et al., 2017. Half a degree additional warming, prognosis, and projected impacts (HAPPI):  
611 background an experimental design, *Geosci. Model Dev.*, 10:571-583, 10.5194/gmd-10-571-2017

612 Neale, R, 2010. Description of the NCAR Community Atmosphere Model (CAM 4.0), NCAR TECHNICAL  
613 NOTE, [http://www.cesm.ucar.edu/models/ccsm4.0/cam/docs/description/cam4\\_desc.pdf](http://www.cesm.ucar.edu/models/ccsm4.0/cam/docs/description/cam4_desc.pdf)

614 O’Gorman P, and Schneider T, 2009. The physical basis for increases in precipitation extremes in  
615 simulations of 21st-century climate change, *Proceedings of the National Academy of Sciences*,  
616 106(35):14773-14777, 10.1073/pnas.0907610106

617 O’Gorman P, Allan R, Byrne M, and Previdi M, 2012. Energetic Constraints on Precipitation Under  
618 Climate Change, *Surv Geophys*, 33:585–608, 10.1007/s10712-011-9159-6

619 Perica, S. and E. Foufoula-Georgiou, 1996. Model for multiscale disaggregation of spatial rainfall based  
620 on coupling meteorological and scaling descriptions, *J. Geophysical Research*, 101(D21), 26:347-361,  
621 10.1029/96JD01870

622 Pfahl S, O’Gorman P, and Fisher E, Understanding the regional pattern of projected future changes in  
623 extreme precipitation, *Nature Climate Change*, 7(6), 10.1038/nclimate3287

624 Rajczak J and Schär C, 2017. Projections of future precipitation extremes over Europe. A multimodel  
625 assessment of climate simulations, *J. Geophys. Res. Atmos.*, 122:10773-10800, 10.1002/2017JD027176

626 Rajczak J, Pall P, and Schär C, 2013. Projections of extreme precipitation events in regional climate  
627 simulations for Europe and the Alpine Region, *J. Geophys. Res. Atmos.*, 118:3610–3626,  
628 10.1002/jgrd.50297

629 Rojas R, Feyen L, Bianchi A, and Dosio A, 2012. Assessment of future flood hazard in Europe using a  
630 large ensemble of bias-corrected regional climate simulations *J. Geophys. Res.: Atmos.*, 117, D17109,  
631 10.1029/2012JD017461

632 Rojas R, Feyen L and Watkiss P, 2013. Climate change and river floods in the European Union: Socio-  
633 economic consequences and the costs and benefits of adaptation. *Glob. Environ. Change* 23:1737–1751,  
634 10.1016/j.gloenvcha.2013.08.006

635 Sillmann J, Kharin B, Zwiers F, Zhang X, and Bronaugh D, 2013. Climate extreme indices in the CMIP5  
636 multi-model ensemble. Part 2: Future projections, *J. Geophys. Res.*, 10.1002/jgrd.50188

637 Scoccimarro E, Gualdi S, Bellucci A, Zampieri M, Navarra A, 2016. Heavy precipitation events over the  
638 Euro-Mediterranean region in a warmer climate: results from CMIP5 models. *Reg Environ Change*, 16:  
639 595, 10.1007/s10113-014-0712-y

640 Schaller et al., 2016. Human influence on climate in the 2014 southern England winter floods and their  
641 impacts, *Nature Climate Change*, DOI:10.1038/nclimate2927

642 Stone D and Pall P, in preparation, A benchmark estimate of the effect of anthropogenic emissions on the  
643 ocean surface

644 Thober S, Kumar R, Wanders N, Marx A, Pan M, Rakovec O, Samaniego L, Sheffield J, Wood E, and  
645 Zink M, 2018. Multi-model ensemble projections of European river floods and high flows at 1.5, 2, and 3  
646 degrees global warming, *Environ. Res. Lett.*, 13,014003, 10.1088/1748-9326/aa9e35

647 Wehner M, Reed K, Loring B, Stone D, and Krishnan H, 2018. Changes in tropical cyclones under  
648 stabilized 1.5°C and 2.0°C global warming scenarios as simulated by the Community Atmospheric Model  
649 under the HAPPI protocols. *Earth System Dynamics*, 9:187-195, 10.5194/esd-9-187-2018

650 Westra S., Brown C., Lall U., Sharma A, 2007. Modeling multivariable hydrological series: Principal  
651 component analysis or independent component analysis?, *Water Resources Research*, 43(6),  
652 10.1029/2006WR005617

653 Winsemius H, Aerts J, van Beek L, Bierkens M, Bouwman A, Jongman B, Kwadijk J, Ligtoet W, Lucas P,  
654 van Vuuren D, and Ward P, 2016. Global drivers of future river flood risk, *Nature Climate Change*, 6:381-  
655 385, 10.1038/nclimate2893

656 Vautard R, Gobiet A, Sobolowski S, Kjellström E, Stegehuis A, Watkiss P, Mendlik T, Landgren O, Nikulin  
657 G, Teichmann C, and Jacob D, 2014. The European climate under a 2 C global warming, *Environ. Res.*  
658 *Lett.*, 9,034006, 10.1088/1748-9326/9/3/034006

659 UNFCCC, 2015. Adoption of the Paris agreement, Proposal by the President Technical report (Geneva:  
660 United Nations) (<http://unfccc.int/resource/docs/2015/cop21/eng/l09r01.pdf>)

661 UN, 2017. World Population Prospects, The 2017 Revision, Key Findings and Advance Tables.  
662 [https://esa.un.org/unpd/wpp/publications/files/wpp2017\\_keyfindings.pdf](https://esa.un.org/unpd/wpp/publications/files/wpp2017_keyfindings.pdf)

663 Zanardo, S., Nicotina, L., Hilberts, A. G. J., & Jewson, S. P. (2019). Modulation of economic losses from  
664 European floods by the North Atlantic Oscillation. *Geophysical Research Letters*, 46.  
665 10.1029/2019GL08195

666

667

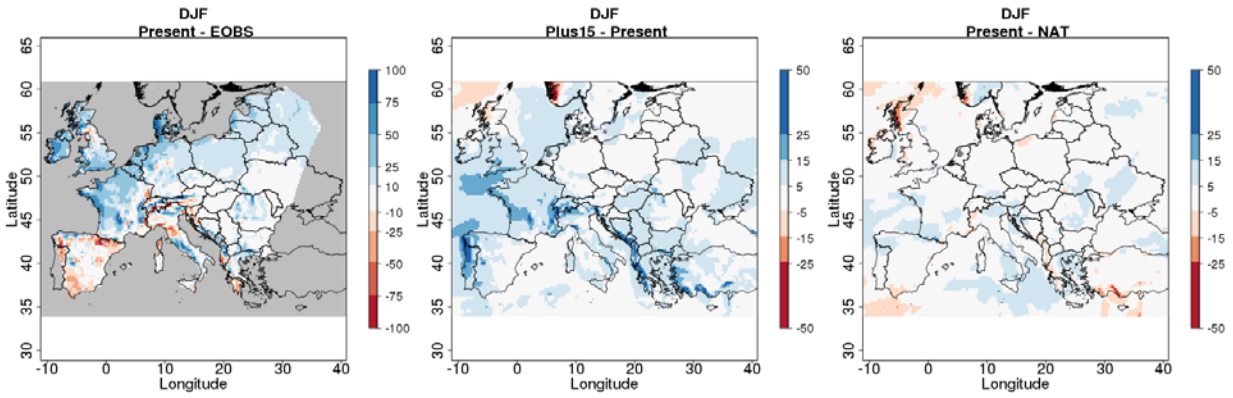
668

669

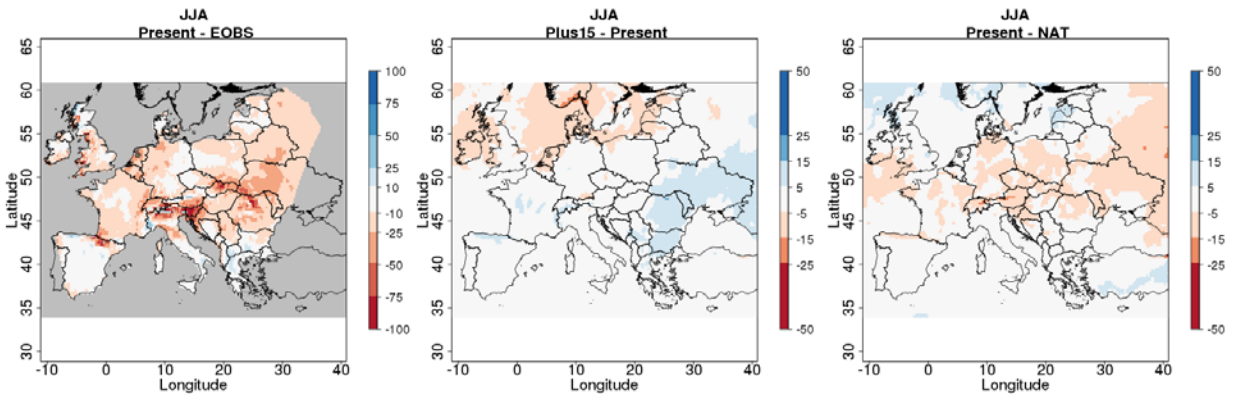
670



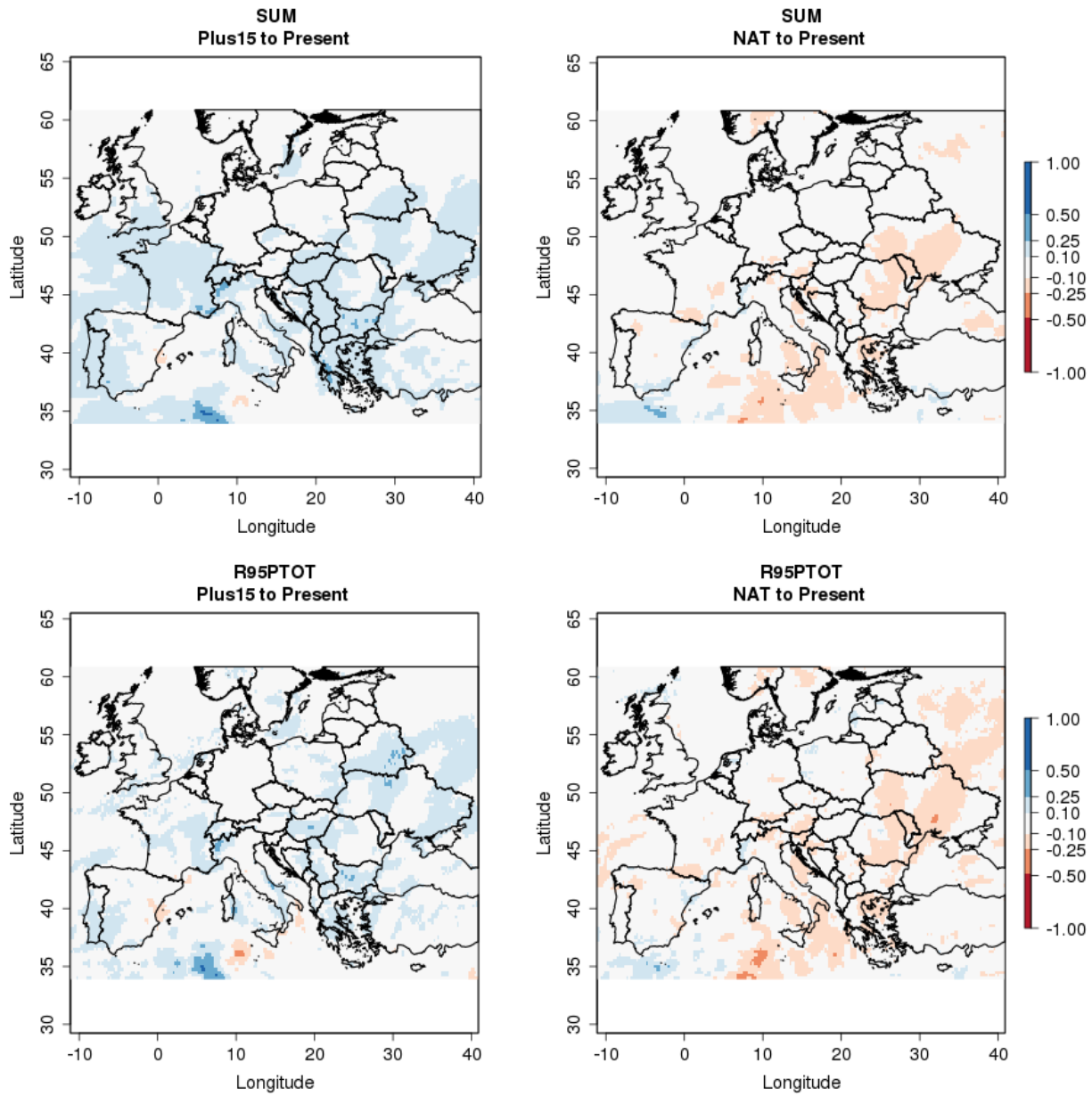
671



672

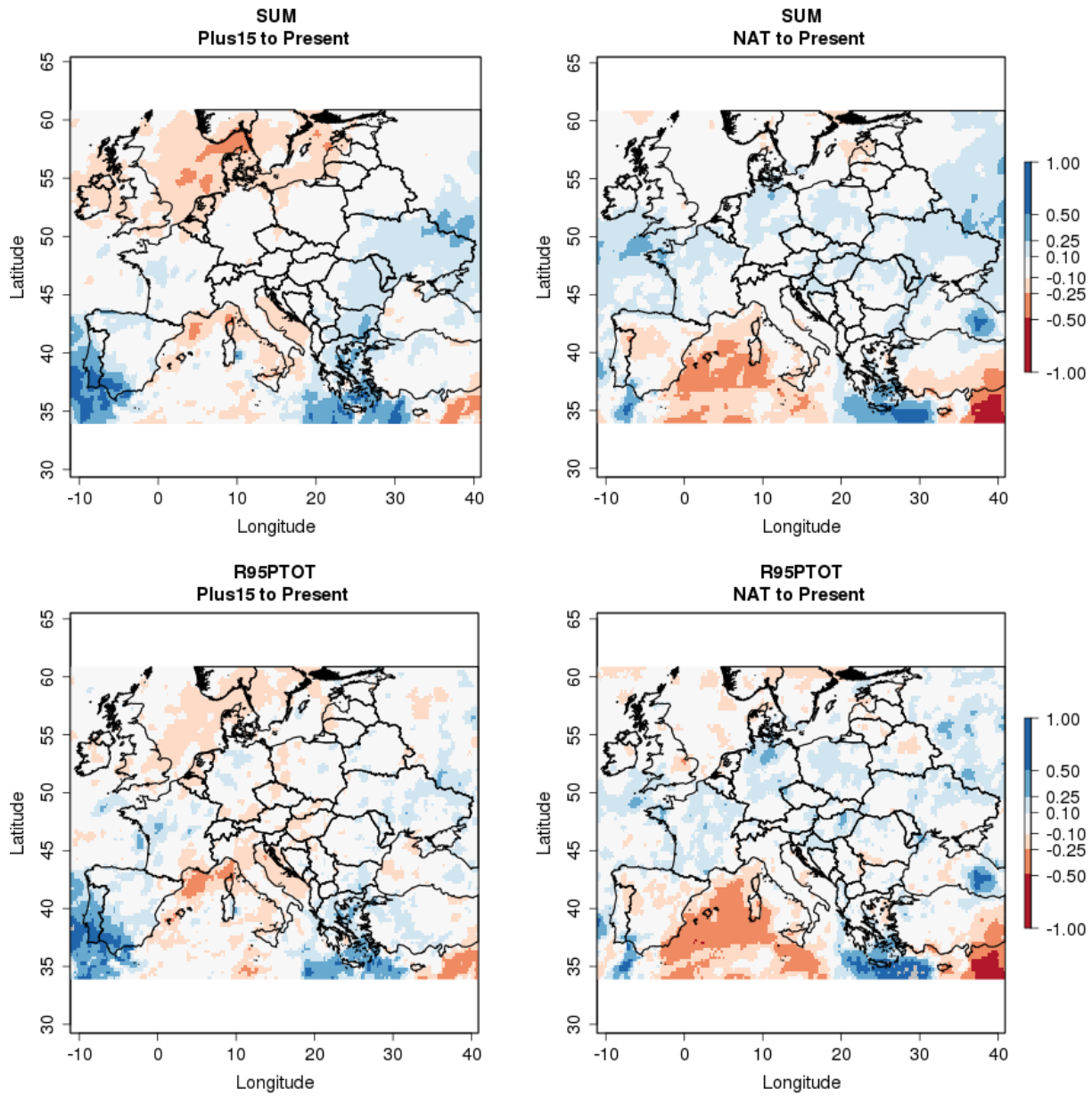


673 Figure 1. Difference of mean winter precipitation (top) and mean summer precipitation (bottom) for  
674 Present minus E-OBS (period 1961-2011), Plus15 minus Present and Present minus NAT scenarios;  
675 units are in mm.



676

677 Figure 2. Relative change of winter total precipitation and R95pTOT for future climate (Plus15) and  
 678 natural climate (NAT).



679

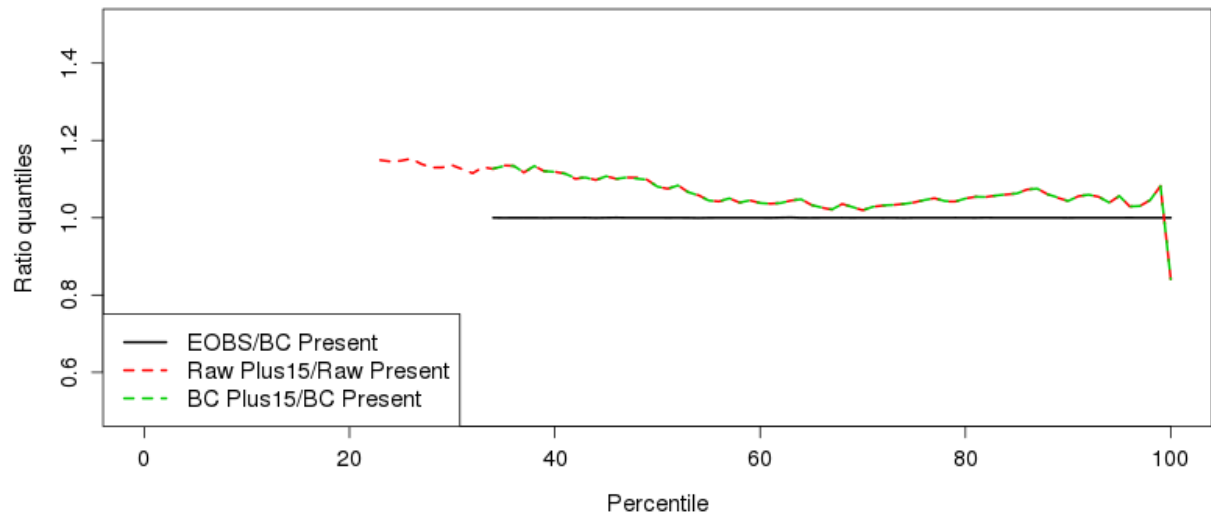
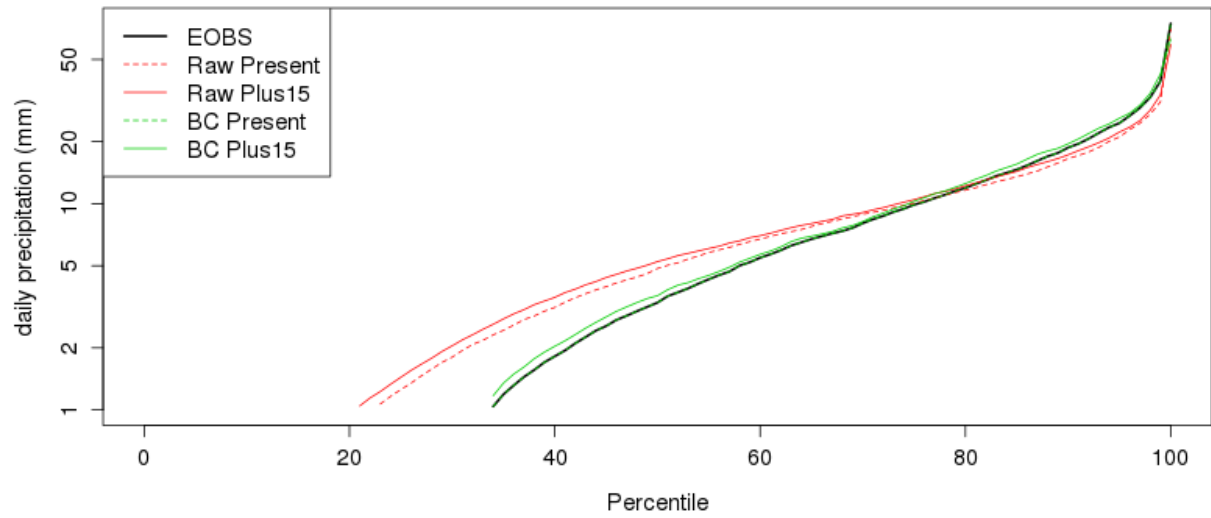
680 Figure 3. Relative change of summer total precipitation and R95pTOT for future climate (Plus15) and  
 681 natural climate (NAT).

682

683

684

685



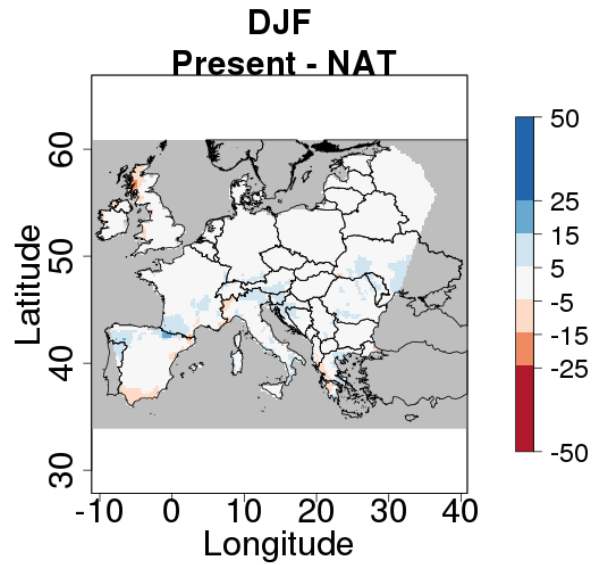
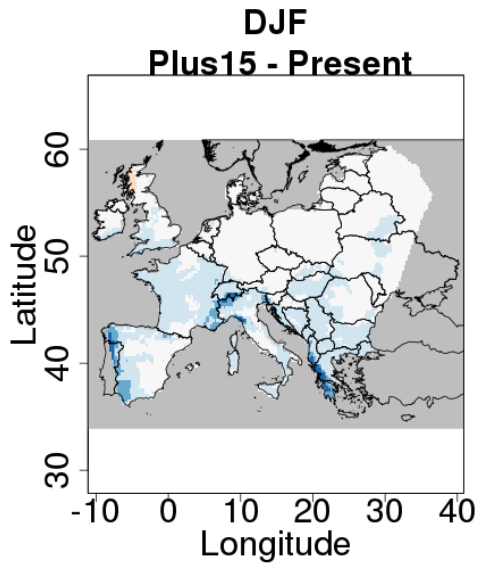
686

687 Figure 4. Example of cumulative distributions of winter daily precipitation for E-OBS (period 1961-2011),  
 688 raw simulations and bias-corrected simulations.

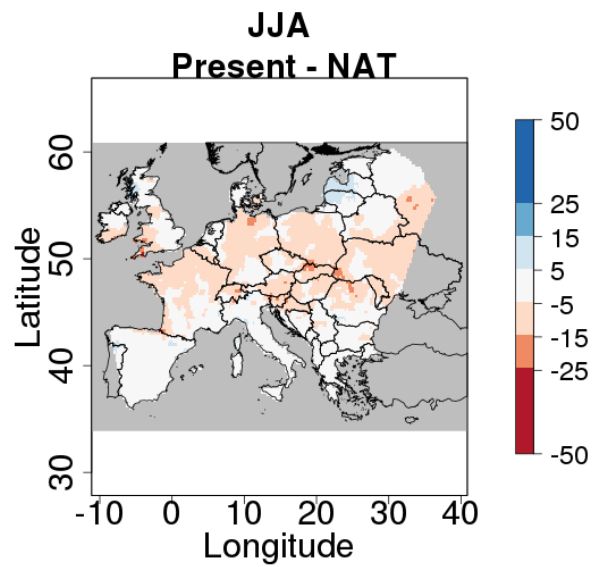
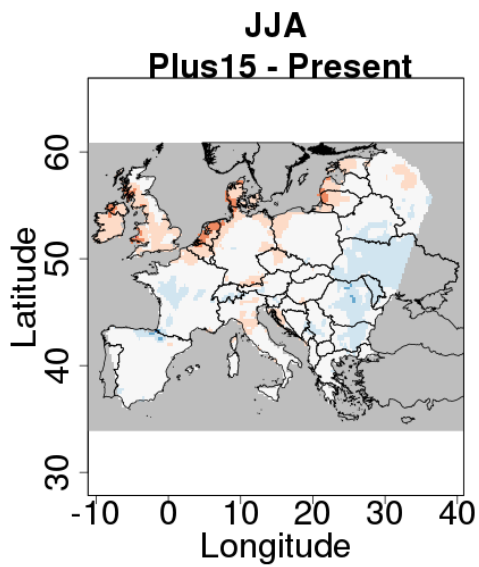
689

690

691

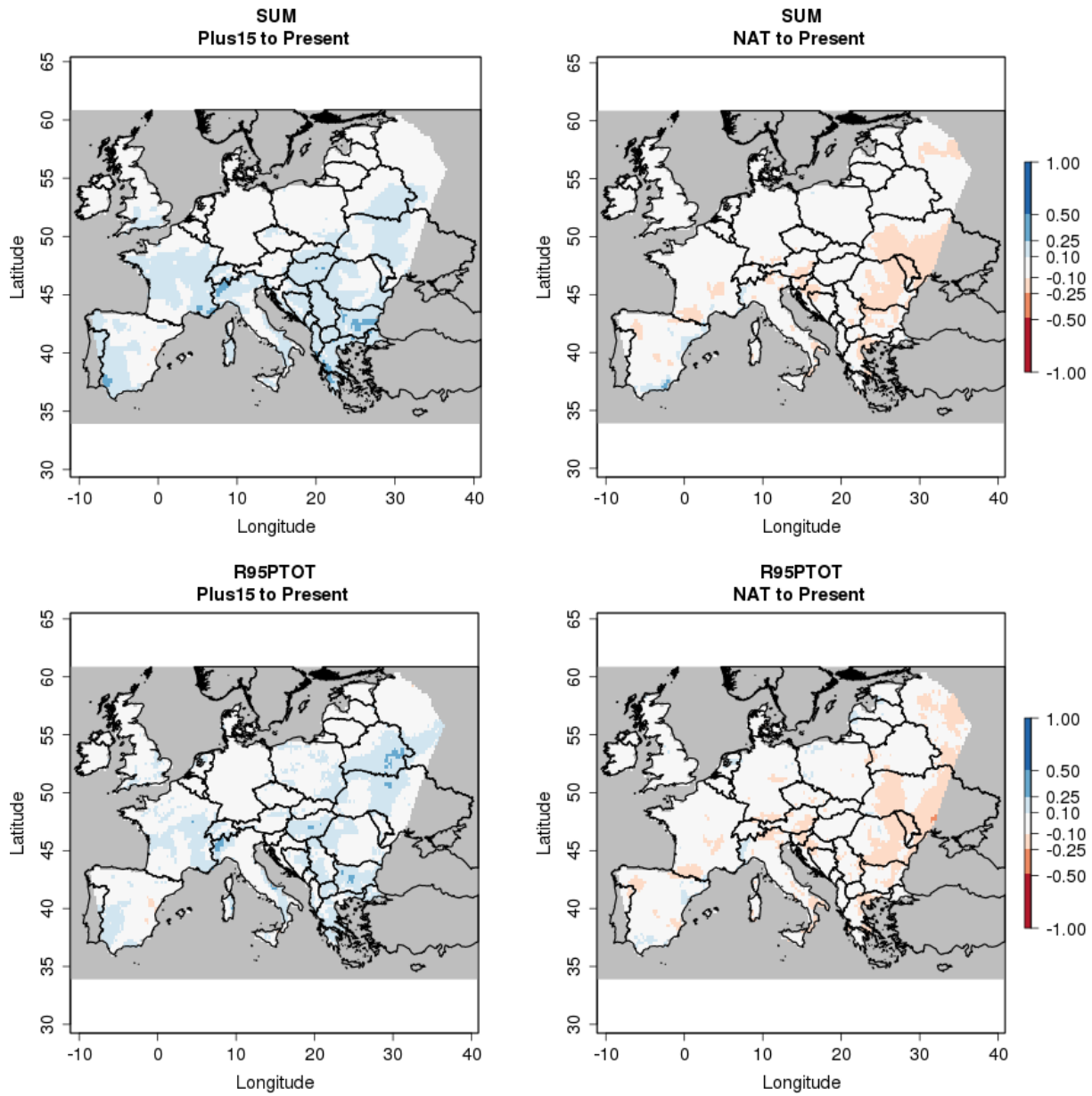


692



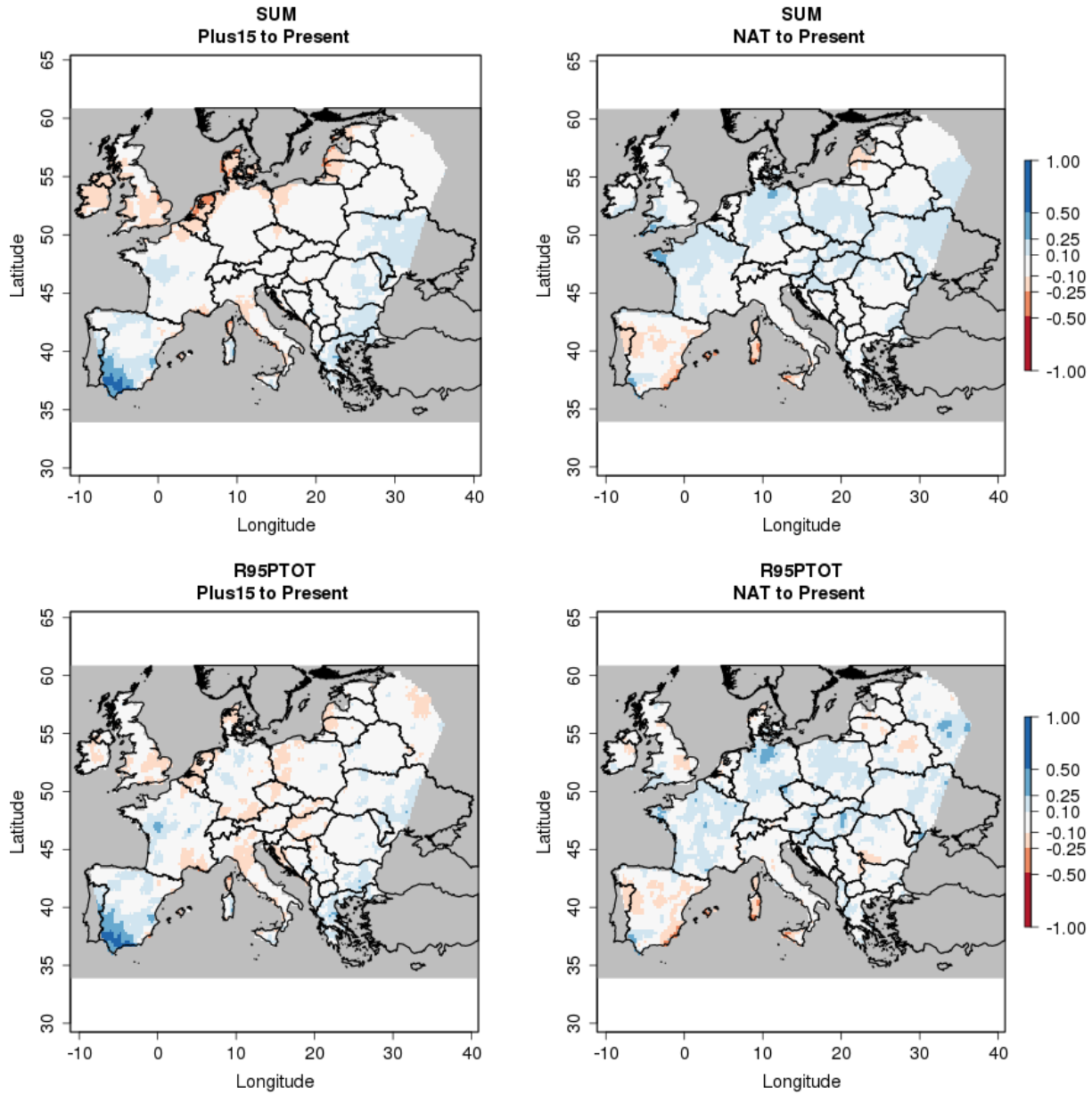
693

694 Figure 5. Difference of mean winter precipitation (top) and mean summer precipitation (bottom) for Plus15  
695 minus Present and Present minus NAT scenarios, after bias-correction; units are in mm.



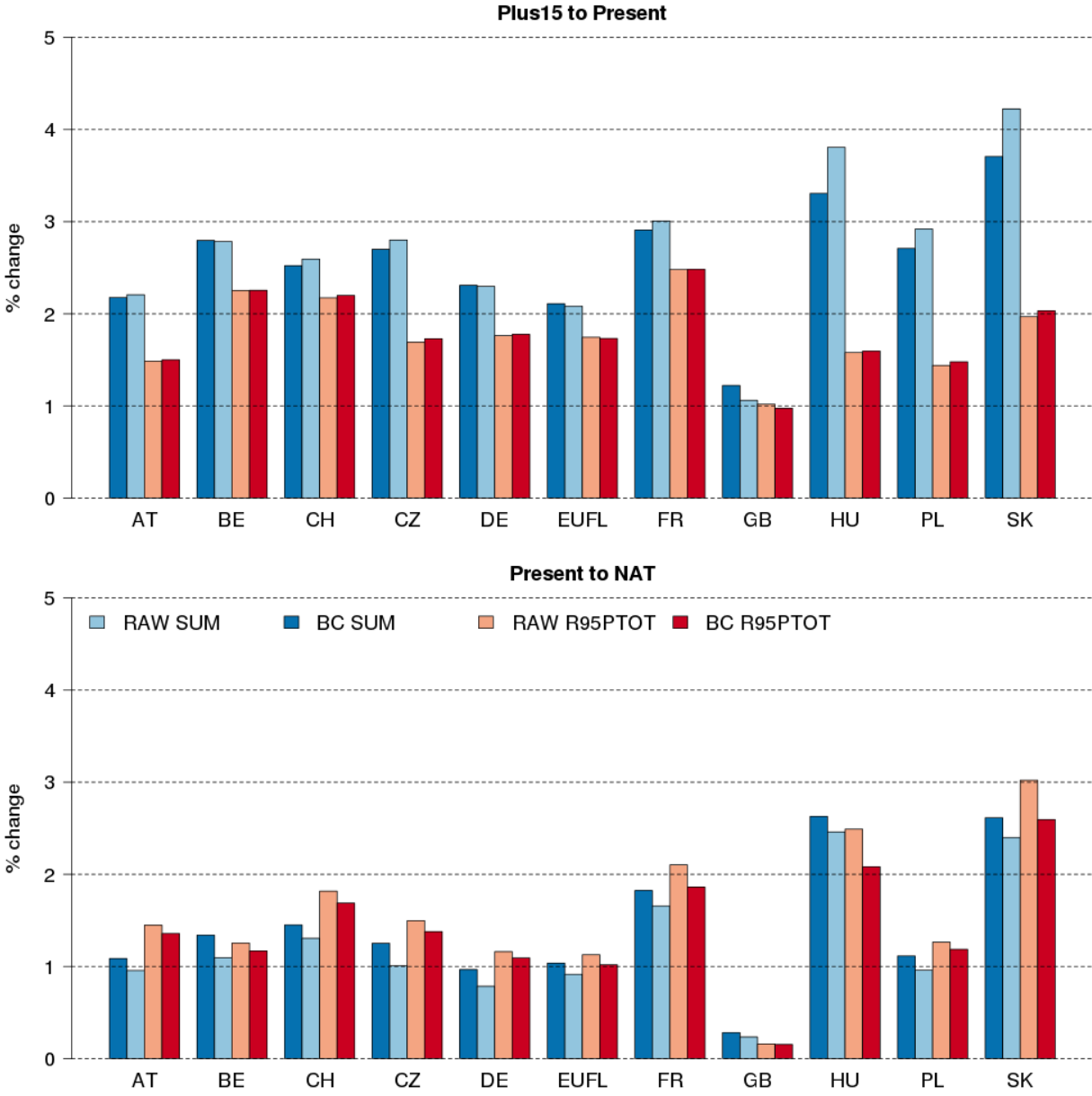
696

697 Figure 6. Relative change of winter total precipitation (SUM) and R95pTOT for future climate (Plus15) and  
 698 natural climate (NAT) after bias-correction.



699

700 Figure 7. Relative change of summer total precipitation (SUM) and R95pTOT for future climate (Plus15)  
 701 and pre-industrial climate (NAT) after bias-correction.



702

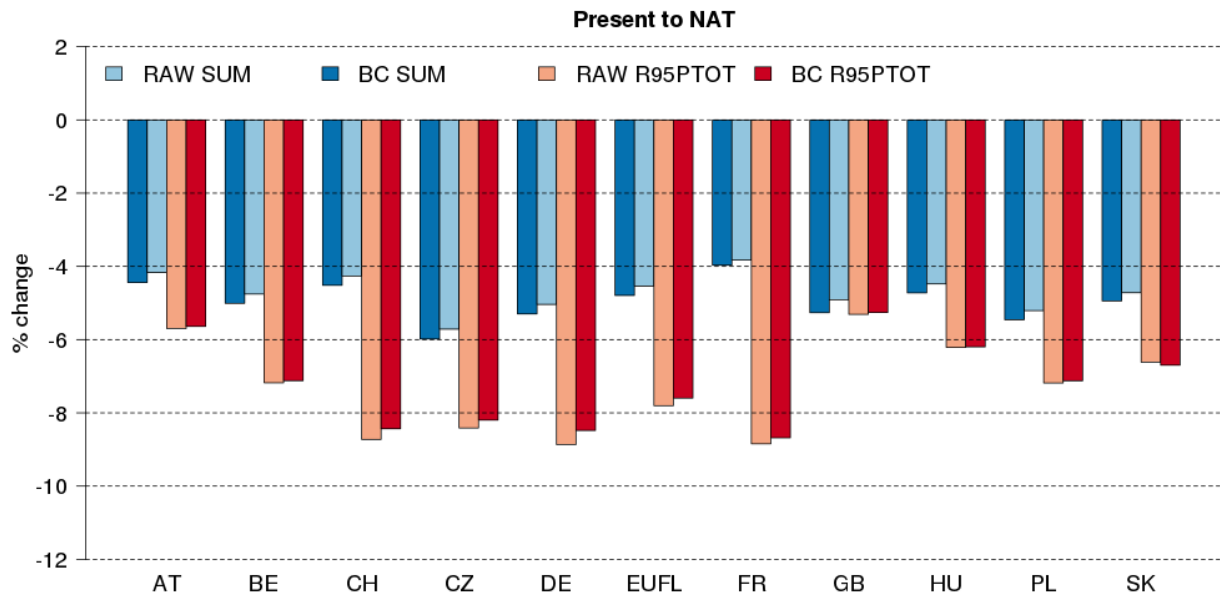
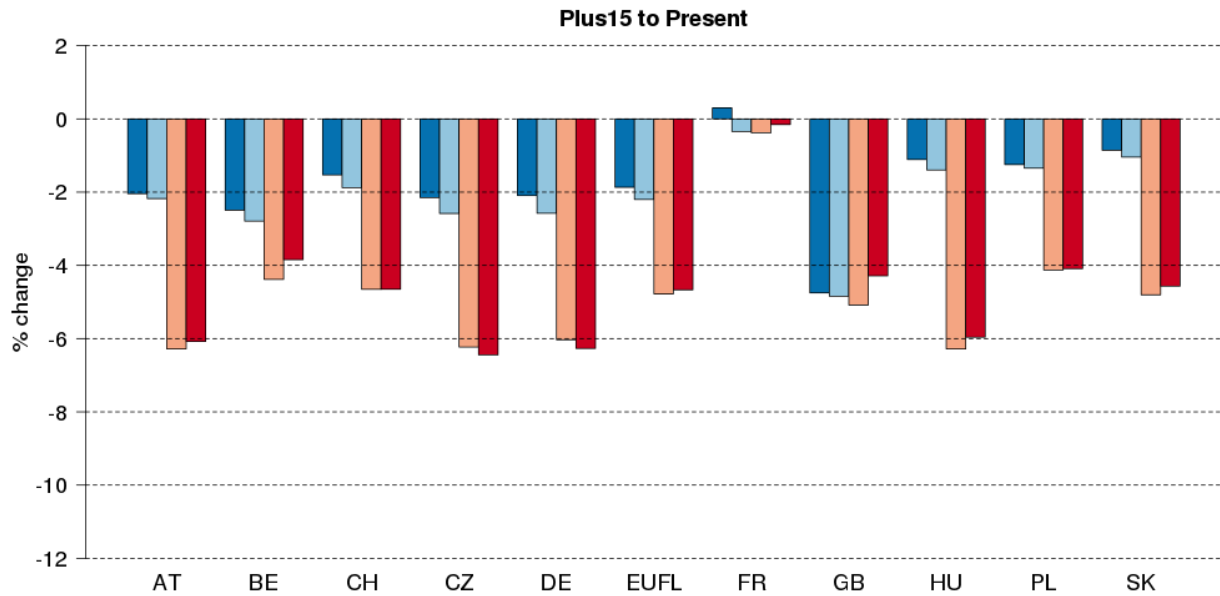
703

704

705

Figure 8. Relative change in winter losses expressed as percentage change per decade by country and for the entire domain (denoted with EUFL), based on the relative change in the raw and bias-corrected precipitation statistics for the Plus15 and NAT scenarios.





706

707 Figure 9. Relative change in summer losses expressed as percentage change per decade by country and  
 708 for the entire domain (denoted with EUFL), based on the relative change in the raw and bias-corrected  
 709 precipitation statistics for the Plus15 and NAT scenarios.